Journal of Structural Geology, Vol. 10, No. 2, pp. 201 to 209, 1988
Printed in Great Britain

0191-8141/88 $03.00 + 0.00

Normalized center-to-center strain analysis of packed aggregates

ERIC A. ERSLEV

Department of Earth Resources, Colorado State University, Fort Collins, CO 80523, U.S.A.

(*Received* 6 *July* 1987; *accepted in revised form* 30 *November* 1987)

Abstract—The resolution of conventional techniques of center-to-center strain analysis is limited by the degree of original anticlustering of centers on the analyzed plane. However, the three-dimensional anticlustering of packed objects does not result in equivalent anticlustering on two-dimensional planes through these aggregates. Size variations due to imperfect sorting further decrease the anticlustering of natural aggregates. For the Fry all-object-object separations method, these problems are manifested in vague point-density distributions and ambiguously defined strain ellipses.

Normalization of center-to-center distances allows more precise determination of small initial and tectonic anisotropies in packed aggregates. On planes through packed aggregates, object spacing is a function of object size, shape and the distance between object margins. Dividing the center-to-center distance between two objects by the sum of their average radii eliminates variations due to object size and sorting. Analyses of synthetic aggregates of packed spheres and statically recrystallized iron show that normalized Fry diagrams form better-defined vacancy fields and sharper rims of maximum point density regardless of the original sorting and anticlustering in the aggregate. Normalized strain analyses of deformed aggregates also show greatly increased resolution, with variable initial and tectonic ellipticity resulting in a wider ring of high point-density.

INTRODUCTION

ONE OF the great advances in structural geology during the last decade has been the quantification of deformation by the measurement of rock fabric. The analytical analysis of micro- and macro-fabric has potential applications in all fields that utilize petrographic observations. However, the low resolution of many methods of strain analysis prevents wider application of these techniques. This paper will show that normalization of fabric data by object size can greatly increase the resolution of center-to-center strain analyses by eliminating the necessity for two-dimensional anticlustering. The advantages of normalizing center-to-center distances will be developed for the simple case of undeformed aggregates and then generalized to the deformed case.

Ramsay (1967, p. 195) recognized that distances between the centers of adjacent objects in a rock can be used to quantify finite strain if these objects were initially distributed equally through the rock. His technique involves plotting the distances between the centers of nearest neighbors vs the angles defined by the lines between centers and a reference line. Unfortunately, difficulties of measurement and interpretation have resulted in minimal application of Ramsay's method. Fry (1979) proposed the all-object-object separations method, now known as the *Fry method*, where the relative positions of adjacent grains are directly plotted by sequentially putting the origin of an overlay on each center and recording the position of adjacent centers as points. In many aggregates, these points define an elliptical void and parallel ring of high point-density around the origin of the overlay. These ellipses will equal the finite-strain ellipse for homogeneously deformed populations of originally statistically-uniform centers. The advantage of Fry's method lies in the ease and rapidity of analysis and interpretation, although the definition of the strain ellipse is often weak and ambiguous due to clustering of the centers.

LIMITATIONS ON TWO-DIMENSIONAL ANTICLUSTERING

Ramsay & Huber (1983) described anticlustered aggregates as points that are distributed in such a way that the distances between them are more or less constant. The importance of anticlustering was emphasized by Fry (1979) who demonstrated that deformation of a random Poisson distribution of centers results in an equally random and uninterpretable array of center-to-center distances. Using the Fry method, Crespi (1986) showed that more centers are needed to accurately define the strain ellipse in poorly anticlustered aggregates. However, it is important to realize that even perfect three-dimensional anticlustering in a body does not result in equivalent anticlustering on the two-dimensional surfaces used for strain analysis.

This critical fact is demonstrated by the sections through synthetic, undeformed aggregates of packed spheres and polygons (Fig. 1). The spherical symmetry of these and other undeformed aggregates provides a known, simplified reference state that will be extrapolated to a more generalized elliptical geometry later in the paper. In both cases illustrated in Fig. 1, equal object spacings and volumes in three-dimensions necessitate neither equal spacings nor areas in two-dimensions. This results in a reduction of anticlustering going from three- to two-dimensions. Figure 1(a) shows a random slice through equal-sized spheres from Graton & Fraser (1935), analogous to a two-dimensional slice through a perfectly-sorted sandstone composed of spherical

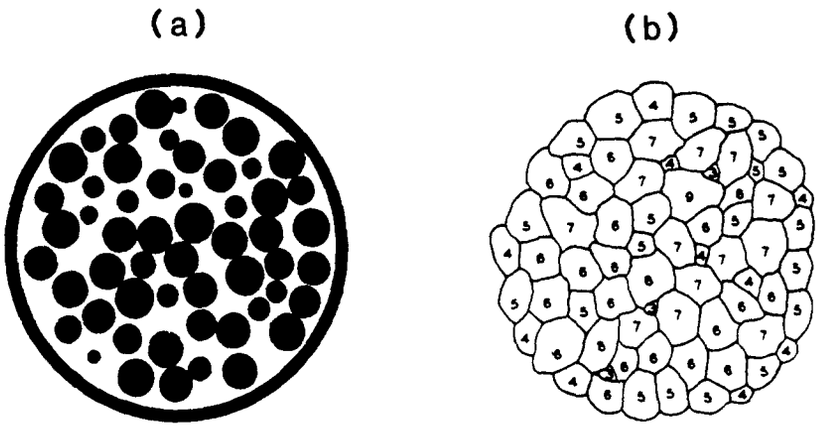

Fig. 1. Random sections through (a) packed, equal-volume spheres (from Graton & Fraser 1935) and (b) three-dimensional polygons (from Smith 1964; inscribed numbers refer to the number of faces on each polygon). Note the limited anticlustering in two-dimensions even though these aggregates approach perfect anticlustering in three-dimensions.

grains. In three-dimensions, the centers of nearest-neighbor spheres are separated by a constant distance equaling two times the radius of the spheres, resulting in perfect anticlustering. In contrast, distances between the centers of adjacent circles in Fig. 1(a), defined by the intersection of the plane with the packed spheres, are obviously not constant.

The slice through crystalline polygons in Fig. 1(b), used by Smith (1964) to illustrate variability in cross-section area on planes through grains with equal volumes, shows a considerable range of distances between nearest neighbor centers. In three-dimensions, the distances between the centers of nearest neighbor polygons should be approximately equal. Once again, the distances between the centers of adjoining grains in a plane are not equal because these chords only rarely connect the true, three-dimensional centers of the objects.

This diminution of anticlustering going from two- to three-dimensions is due to the fact that relatively few three-dimensional centers of objects will be contained in a thin section or on the surface of a slab (see Bhattacharyya & Longiaru 1986, for a parallel discussion). For instance, a thin-section of an oolitic limestone will contain sections through the ends of ooliths as well as principal sections containing the actual three-dimensional centers of the ooliths. If the principal section of an oolith does occur on the examined surface, adjacent oolith sections probably will not contain their three-dimensional centers. Thus, the actual distances measured in conventional center-to-center analyses are the distances between the central axes of the ooliths, not the distances between their centers.

PACKING AND NORMALIZATION OF CENTER-TO-CENTER DISTANCES

Three-dimensional anticlustering in rocks usually results from the packing of objects with similar volumes. This uniformity of object size commonly results from hydrologic sorting, crystallization kinetics or metastable textural equilibrium. Anticlustering of packed aggregates occurs due to the fact that grains cannot physically overlap. In the case of packed spheres in contact with each other in three-dimensions, the shortest distance between two centers equals the sum of their radii.

In two-dimensions, a planar surface intersecting packed spheres defines small circles with radii ranging from that of the intersected spheres to zero. The center-to-center distance between two adjacent small circles equals the sum of their radii plus the minimum distance between the margins of the circles. This suggests an alternative approach to characterizing two-dimensional center-to-center distances. Normalizing the center-to-center distance between two small circles by dividing by the sum of their radii (equation 1) eliminates the object size (quantified in this case by the circle radii) variable.

For small circles a and b, the normalized distance between their centers is:

$$D_n = D/(r_a + r_b); \quad (1)$$

where r_a, r_b = radii of small circles a and b, and D = distance between centers of small circles a and b.

As the distance between small circles decreases, the center-to-center distance approaches the sum of the radii between the two objects and the normalized distance approaches one. Small circles that touch have the minimum normalized distances of one, regardless of their radii. Thus, this normalization will also remove variations due to imperfect original sorting of the spheres. Small circles not in contact will have distances greater than one.

Theoretical frequency distributions of center-to-center distances demonstrate the advantages of normalizing distances using equation (1). The radial symmetry of packed, equal-volume spheres allows the projection of the three-dimensional geometry along the z axis, resulting in the two-dimensional geometry summarized in Fig. 2(a). One sphere was fixed with its center at the origin and its position was compared to nearest neighbor spheres of equal diameter in contact with the fixed sphere at one point on the x–y plane. These spheres were intersected by 39 equally spaced planes paralleling

the x–z plane and representing all possible planes of analysis viewed on end.

To simulate distances from the origin of a conventional Fry diagram, the distance between the centers of the small circles intersected by each of the planes was recorded in a cell of a computer spreadsheet. This procedure was repeated for 89 equally-spaced, nearest neighbor spheres in contact with the fixed sphere, resulting in a matrix of center-to-center distances. The spreadsheet algorithm is summarized below, with distances calculated using equation (2) and their frequency distribution shown in Fig. 2(b).

For $\theta = 0.5$ to 88.5° (1° increments) and $H = 0.999$ to -0.951 (0.05 increments), if $H < y - 1$, then D is undefined (plane does not intersect both spheres), if $H \geq y - 1$, then

$$D = x = 2 * \sin \theta, \quad (2)$$

where x,y = co-ordinates of the center of a nearest neighbor sphere, θ = angle from the y axis of the line from 0,0 to x,y, $H = y$ co-ordinate of intersecting plane and D = distance between small circle centers on the intersecting plane.

Distances normalized using equation (1) were calculated using the same spreadsheet matrix with the distance algorithm in equation (3), resulting in the frequency distribution in Fig. 2(c).

$$D_n = D/(r_a + r_b) \quad (1)$$

$$= 2 * \sin \theta/((1 - H^2)^{1/2} + (1 - (2 * \cos \theta - H)^2)^{1/2}), \quad (3)$$

where $D = 2 * \sin \theta$, and $r_a = (1 - H^2)^{1/2}$, $r_b = (1 - (2 * \cos \theta - H)^2)^{1/2}$ (by the Pythagorean Theorem).

The peak heights of the frequency diagrams in Fig. 2 are very similar, with peak shapes showing exponential increases of opposite slope. The conventional Fry method generates a distance maximum at two times the radius of the spheres because more planes intersect both spheres when the line between their centers parallels the planes of analysis. For normalized distances, the frequency maximum occurs at the minimum normalized distance of one which is achieved for all planes containing the contact between the spheres. Thus, the distance maxima of these two frequency diagrams contain different distances. Distances that enhance the frequency maximum of normalized center-to-center distances (e.g. the plane closest to the contact of the shaded sphere with the fixed sphere in Fig. 2a) usually detract from sharpness of the frequency maximum of unmodified distances (and thus the resolution of the conventional Fry technique) by occupying the zone between the frequency maximum and zero. These distances will plot within the rim of maximum point-density on a Fry diagram, masking the definition of the vacancy field. Likewise, the center-to-center distances between spheres whose centers are aligned parallel to the plane of analysis do not necessarily add to the resolution of the normalized Fry method.

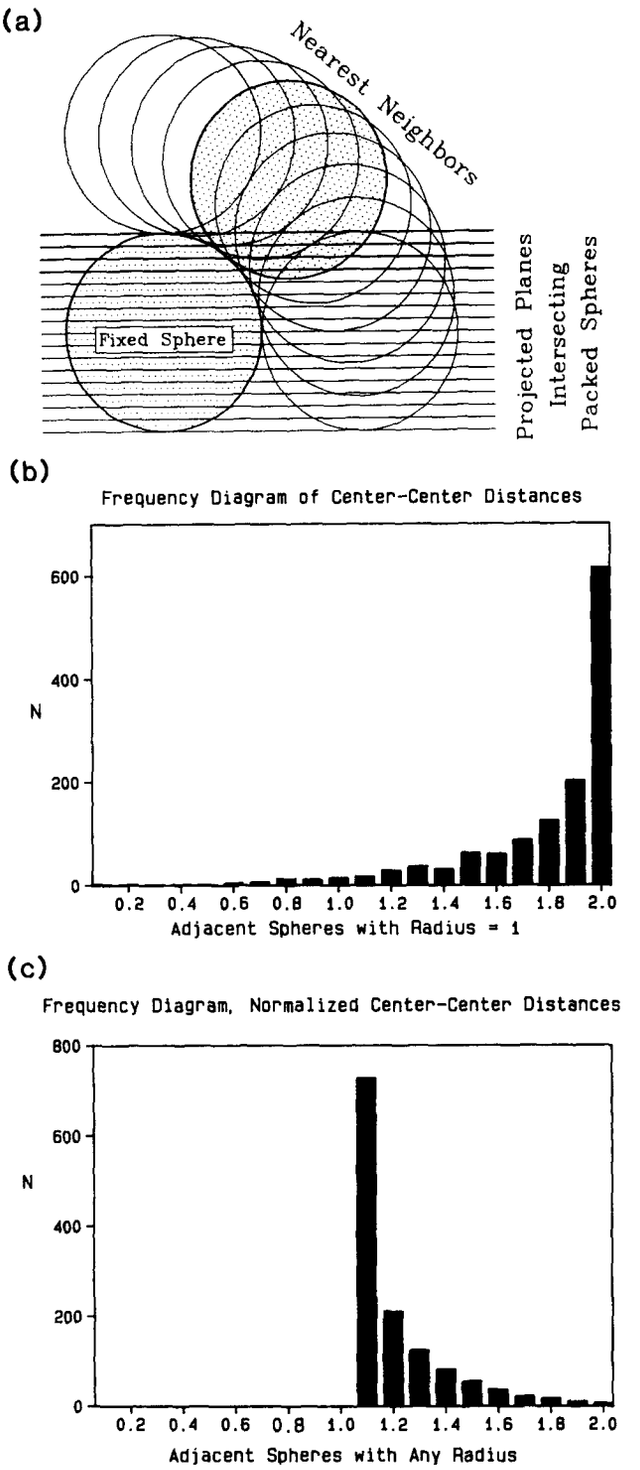

Fig. 2. (a) Diagram representing the theoretical simulation of all possible planes intersecting a fixed sphere in grain contact with nearest neighbor spheres of equal volume (see text for algorithms). The following frequency diagrams were generated by calculating center-to-center distances on the equally-spaced planes for the fixed sphere and each nearest neighbor sphere. (b) Frequency distribution of center-to-center distances using equation (2). (c) Frequency distribution of center-to-center distances normalized by the sum of the radii of the small circles intersected by each plane (equation 3).

These frequency diagrams show two important advantages of normalizing by the sum of the small circle radii when plotting all-object-object separation diagrams. First, the vacancy field in normalized Fry center-to-center analysis will be much better defined, with the abrupt increase in point density from zero to the

maximum allowing clearer definition of the ring of maximum point density. The shape of the void more accurately reflects the bulk strain since it is defined by a greater proportion of the center-to-center distances. Secondly, *the frequency distribution and values of normalized distances are independent of grain size, allowing equal accuracy in both well-sorted and poorly-sorted aggregates of equal sphericity.* In conventional methods of center-to-center strain analysis, variable grain size will result in the superposition of frequency distributions with different maxima, destroying the definition of the point maxima used to define the strain ellipse. For instance, a packed aggregate with two grain sizes (r_1, r_2) will result in three overlapping point distributions with peak maxima at $2 * r_1$, $2 * r_2$ and $r_1 + r_2$ on a conventional Fry diagram. Normalization of each distance using equation (1) will center each of these maxima at 1.

Normalization of center-to-center distances can also be applied to crystalline aggregates without growth-determined shape anisotropy (e.g. Fig. 1b), since equant crystalline polyhedra will approximately inscribe spheres. However, planes intersecting the pointed ends of the polyhedra, which will occupy the interstices between inscribed spheres, will result in a larger proportion of smaller sections through the objects. This will increase the proportion of center-to-center distances significantly less than two times the three-dimensional radii of the inscribed spheres, decreasing the definition of the central vacancy field of a conventional Fry diagram but not affecting the resolution of a normalized Fry diagram.

APPLICATION TO UNDEFORMED PACKED AGGREGATES

Figures 3 and 4 show the superior resolution of the normalized Fry method applied to synthetic aggregates of packed spheres and recrystallized iron. It should be emphasized that the experimental approach used here is completely different from the approaches of Fry (1979), Crespi (1986) and Onasch (1986) who used random number generators to create anticlustered point populations. I concur with Bhattacharyya & Longiaru (1986) who warned that such populations are not realistic analogs for two-dimensional surfaces through natural aggregates. In this study, the co-ordinates of the two-dimensional center and a radius end-point for each object were determined from digitized data and entered into a personal computer program that generates both conventional and normalized Fry plots from the same data set. The radial symmetry of the undeformed aggregates analyzed in Fig. 3 allowed the construction of corresponding frequency diagrams for conventional (column 1 in Fig. 4) and normalized (column 2 in Fig. 4) center-to-center distances analogous to the theoretical distributions in Fig. 2.

Synthetic aggregates of packed spheres, embedded in fiberglass resin, were used to test and compare the center-to-center methods. Spheres of uniform size were used in the aggregate analyzed in Figs. 3(a) and 4(a), whereas three sizes of spheres were used in the aggregate analyzed in Figs. 3(b) and 4(b). These aggregates were cut, polished and photographed, avoiding edge effects by not including spheres adjacent to container walls (Graton & Fraser 1935). Three points on the perimeter of each small circle were digitized from photographs of the polished surfaces. The two-dimensional center and radius of each object were calculated using the fact that the perpendicular bisectors of the three chords defined by the three digitized points intersect at the circle center.

Photomicrographs of iron, cold-hammered and then statically recrystallized for 30 h at 700°C (Habraken & de Brouwer 1966), were used as synthetic crystalline aggregates (Fig. 3c). For these non-circular sections of annealed iron grains, which resemble the polygons in Fig. 1(b), centers and radii end-points of the largest circles inscribed by the grains were determined with a template of concentric circles and digitized.

All of the normalized Fry diagrams provide clearer definition of the rim of maximum point density than any of the conventional Fry diagrams, of which only one is readily interpretable. The sharp transitions from central vacancy fields to rims of maximum point density in the normalized Fry diagrams (Fig. 3) are shown as abrupt increases in distances greater than 1 in the frequency diagrams (Fig. 4). The frequency distributions of center-to-center distances predicted in Fig. 2 for perfectly-sorted spheres can be seen in the inner rims of the Fry plots in Fig. 3(a) and the frequency distributions in Fig. 4(a). In the Fry plot of perfectly sorted spheres in Fig. 3(a), the exponential increase of point density from the inner vacancy towards the high-density rim, which blurs the definition of the rim, will occur regardless of the number of centers used in the analysis. Selectively omitting smaller cross-sections will increase the definition of the inner vacancy field of the original Fry technique but will also necessitate more centers over a larger area and add to the subjectivity of the method. Figures 3(b) and 4(b) show that non-perfect sorting can completely obscure the conventional Fry plot, with the distances between the smaller grains defining the geometry of the inner void, whereas the normalized Fry method is unaffected. The normalized method successfully shows the predicted lack of strain in photomicrographs of recrystallized iron in Fig. 3(c), whereas the conventional Fry diagram cannot be accurately interpreted.

APPLICATION TO DEFORMED NATURAL AGGREGATES

The preceding discussion of unstrained aggregates should not be interpreted as indicating that the normalized Fry method will not work for deformed aggregates. Each of the aggregates shown in Figs. 1 and 2(a) and analyzed in Figs. 3 and 4 can be transformed into deformed aggregates by applying a stretch in one direction. For instance, if the spheres in Fig. 1(a) were

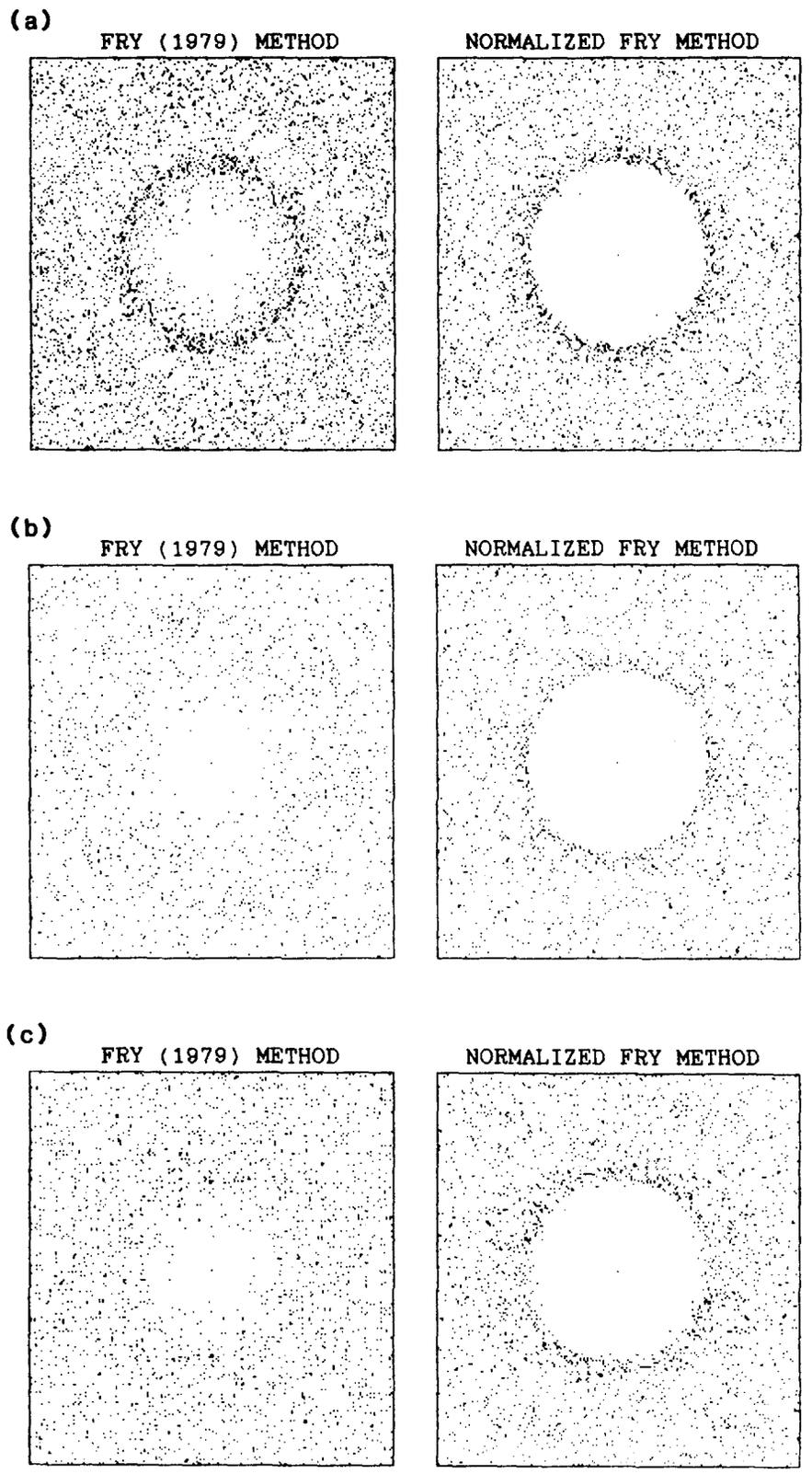

Fig. 3. Fry and normalized Fry center-to-center analyses of (a) 300 equal-sized spheres embedded in fiberglass resin, (b) 180 poorly-sorted spheres embedded in fiberglass resin and (c) 240 annealed iron grains (Habraken & de Brouwer 1966, p. 305).

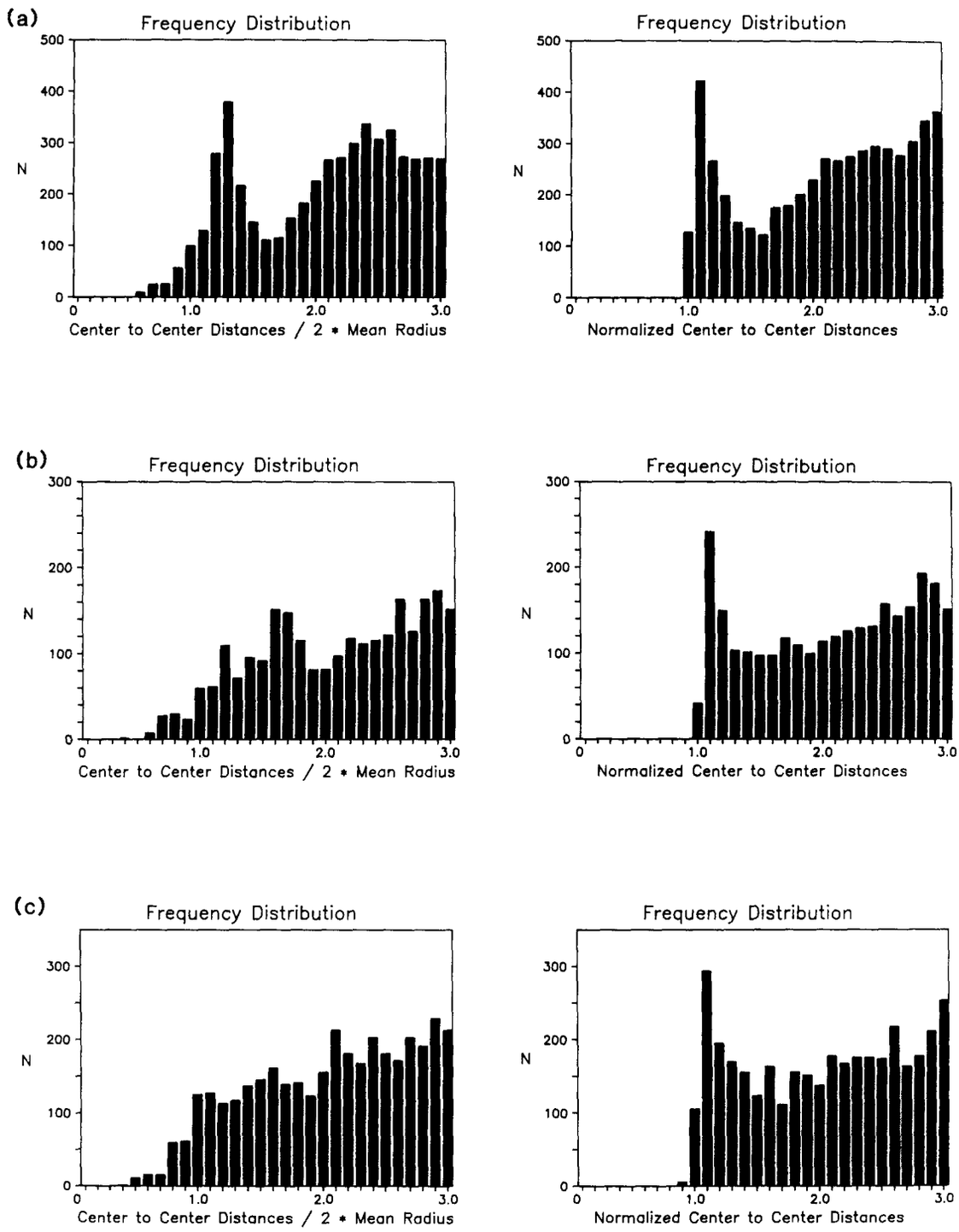

Fig. 4. Frequency diagrams of center-to-center distances and normalized center-to-center distances for the Fry diagrams in Fig. 3. Note the congruence between the theoretical frequency diagrams in Fig. 2 and those of (a).

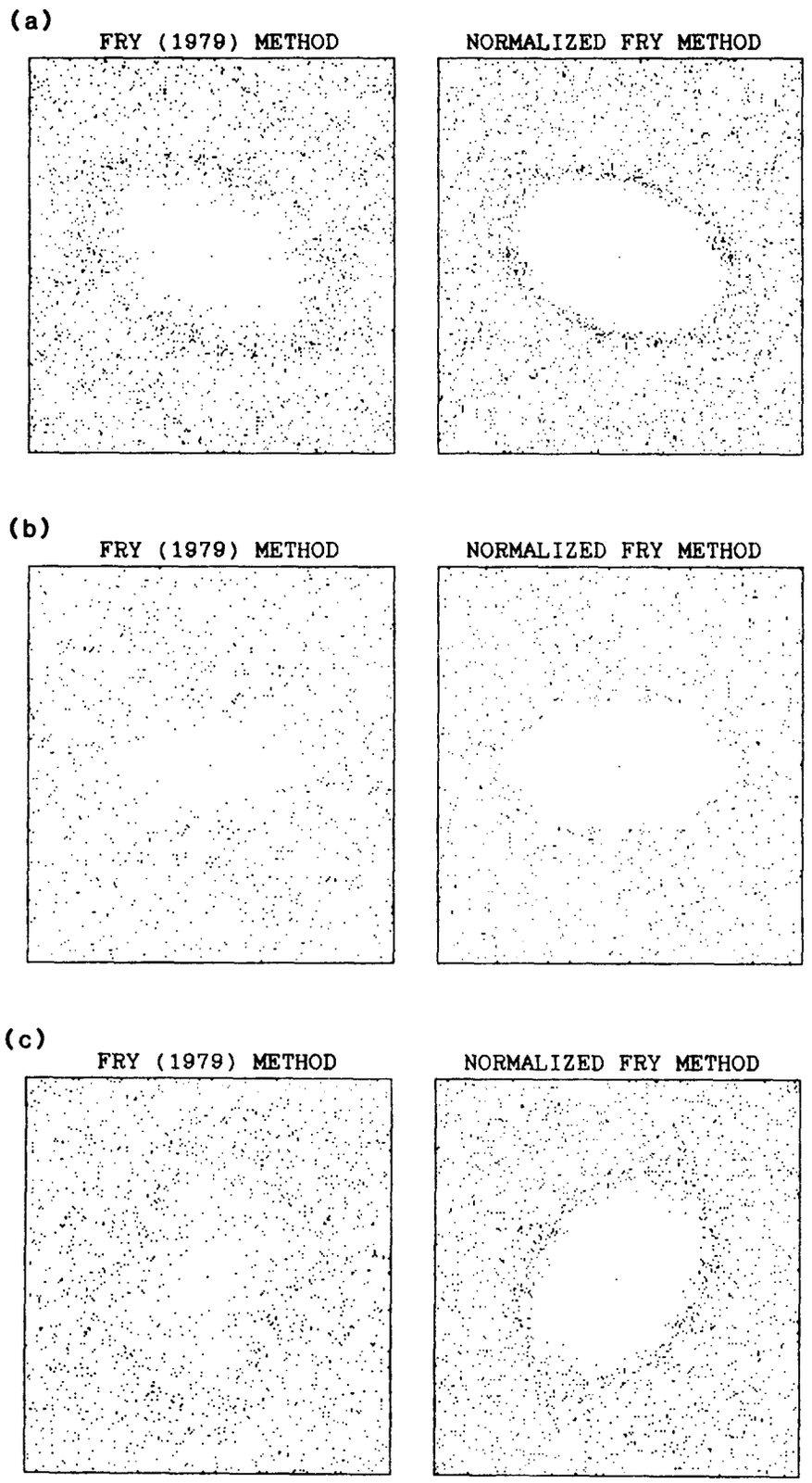

Fig. 5. Comparison of Fry and normalized Fry diagrams for aggregates of 200 deformed objects with variable packing and sorting. (a) Well-sorted, deformed oolitic limestone from fig. 7.7 of Ramsay & Huber (1983). (b) Well-sorted but poorly packed, lapillar tuff from the cover of the 1983 *Journal of Structural Geology* (Vol. 5). (c) More poorly-sorted, deformed oolitic ironstone from fig. 5.7 of Ramsay & Huber (1983).

shortened by 50% in the vertical direction, the vertical component of the center-to-center distances would be halved, resulting in a Fry diagram indicating a strain ellipse with an axial ratio of 2. This is also true for the normalized Fry technique if the radius used for normalization is selected in a consistent manner for all ellipses. If, in the case of the previous example, the horizontal, undeformed radius is chosen to normalize the distances, then the only change to normalization equation (1) will be the change to the center to center distance (D). The resulting normalized Fry plot will also have an elliptical rim of high point-density with the correct axial ratio of 2. If the ellipticity of the objects is approximately constant, normalizing by short axis will also give the same elliptical point distribution since the long axis is related to the short axis by the axial ratio (R). In fact, the distances between ellipse centers can be normalized to any radius as long as they are measured in the same direction for each ellipse.

The effect of local variations in radii can be minimized by normalizing by an average radius defined by the square root of the product of the principal axes of the best-fit ellipse for an object. Assuming that normalization by the long axis (X) is valid and each ellipse has a constant (or nearly constant) axial ratio (R) then the following must hold.

$$\text{Axial ratio} = \text{constant} = R = X_a/Y_a = X_b/Y_b$$

$$\begin{aligned} D_n &= D/(X_a + X_b) \\ &= D/((X_a^2)^{1/2} + (X_b^2)^{1/2}) \\ &= D/((X_a * Y_a * R)^{1/2} + (X_b * Y_b * R)^{1/2}) \\ &= (D/((X_a * Y_a)^{1/2} + (X_b * Y_b)^{1/2})) * 1/R^{1/2} \\ &= (D/((X_a * Y_a)^{1/2} + (X_b * Y_b)^{1/2})) * \text{constant}. \end{aligned} \quad (4)$$

Since the value ($1/R^{1/2}$) is constant for all pairs of objects with equal ellipticity, the effect of normalizing by equation (4) is merely equivalent to changing the scale on the Fry plot. Normalizing by this average radius allows the distribution of deviations due to measurement errors and variable ellipticity. Since the area of an ellipse equals πXY, this effectively normalizes the center-to-center distances by the areas of the ellipses.

For deformed aggregates, best-fit ellipses were calculated for each object by digitizing five points on the margin of elliptical objects and using these points to solve for the equation of a conic. Once the conic was confirmed to describe an ellipse, the center location, ellipticity and angle of inclination of the long axis were calculated using standard techniques to reduce a conic by rotation and translation. The generalized method is described in many analytical geometry texts (e.g. Thomas 1967) and can be easily adapted to computer analysis. This method limits the subjectivity of the determination of the ellipses and allows the integration of center-to-center strain analyses with R_f/ϕ and mean ellipticity calculations.

Figure 5 compares the two center-to-center methods using published photographs of deformed rocks with differing degrees of packing and sorting. For each aggregate, 200 objects were approximated as ellipses using the method described in the preceding paragraph and normalized distances were calculated using equation (4). In Fig. 5(a), analysis of a well-sorted and packed ironstone oolite from Ramsay & Huber (1983, fig. 7.7) resulted in a well-defined ellipse for both methods, with the normalized plot showing better overall definition. The normalized Fry method gives a tightly defined strain ratio (X/Y) of 1.62 which is identical to the harmonic mean (1.62) for this data set and similar to that given by Ramsay & Huber (1983). Figure 5(b) shows center-to-center strain analyses of a poorly-packed lapillar tuff featured on the cover of Volume 5 of the *Journal of Structural Geology* (1983). The normalized Fry method gives a strain ratio of 1.92, which is close to that of the harmonic mean strain ratio of 1.76. The scarcity of adjoining lapilli reduces the definition of both Fry plots, showing the advantage of the better-defined inner vacancy field of the normalized Fry plot.

Figure 5(c) shows center-to-center strain analyses of a poorly-sorted yet well-packed ironstone oolite with variable initial ellipticity from Ramsay & Huber (1983, fig. 5.7). They determined a tectonic strain ratio (X/Y) of 1.7 using the R_f/ϕ method. The normalized Fry method gives a strain ratio of 1.53, whereas the conventional Fry method is difficult to interpret. Because normalization of center-to-center distances using equation (4) essentially recalculates the distances so that each ellipse has an equal area, the discrepancy between the normalized center-to-center and R_f/ϕ methods can be ascribed to the variability of ellipticity in the analyzed surface. The Y axis of the inner rim of maximum point density is determined by the short axis of the most elongated ooliths, whereas the X axis is determined by the long axis of the least elongated ooliths. Therefore, the width of the high point density rim of a normalized Fry plot is a function of variability in ellipticity. This variability can be the result of inhomogeneous deformation or variable initial ellipticity.

DISCUSSION

The simple normalization of the distances between adjacent objects by the sum of their radii can dramatically increase the resolution of center-to-center strain analyses. For packed aggregates, the normalized Fry method eliminates the scatter resulting from imperfectly anticlustered distributions, which can be expected on all two-dimensional surfaces regardless of their degree of three-dimensional anticlustering and sorting. This method allows the evaluation of center-to-center strain in poorly-sorted, recrystallized and weakly-strained aggregates of packed grains. For instance, compaction in sandstones could be measured reliably if large numbers of grains are utilized.

This method will not correct for initial ellipticity or preferred orientation any better than conventional center-to-center methods. However, the increased resolution of normalized center-to-center analysis may provide a tool to investigate initial depositional fabrics

such as the alignment of elongate grains parallel to fluid flow. It will not improve the accuracy of center-to-center analyses in unpacked aggregates such as spaced feldspar phenocrysts or augen. Unlike the conventional Fry method, it cannot be applied directly on an outcrop or slab with a sheet of acetate. However, photographs or tracings of aggregates can be acquired in the field and subsequently digitized in the laboratory.

The test of any method's practicality lies in the ease of its application and interpretation. Thus, even though conventional Fry plots commonly give ambiguous results, the elegant simplicity of the method has made it an important strain technique. Efficient utilization of the normalized Fry method requires a computerized digitizing system for the input of data and calculation of normalized distances. While the acquisition of this hardware was once a major obstacle, the proliferation of inexpensive microcomputers and digitizers has greatly reduced the cost of a work station for computer-aided fabric analysis. The combination of higher resolution methods and low-cost computers promises to make quantitative fabric analysis a standard petrographic procedure for all rocks in the future.

Acknowledgements—This paper has been greatly clarified and improved by comments and reviews by Roy Kligfield, Bob Ratliff, David J. Sanderson, Susan Treagus and two anonymous reviewers.

REFERENCES

Bhattacharyya, T. & Longiaru, S. 1986. Ability of the Fry method to characterize pressure-solution deformation—Discussion. *Tectonophysics* **131**, 199–200.

Crespi, J. M. 1986. Some guidelines for practical application of Fry's method of strain analysis. *J. Struct. Geol.* **8**, 799–808.

Fry, N. 1979. Random point distributions and strain measurement in rocks. *Tectonophysics* **60**, 806–807.

Graton, L. C. & Fraser, H. J. 1935. Systematic packing of spheres—with particular reference to porosity and permeability. *J. Geol.* **43**, 785–909.

Habraken, L. & de Brouwer, J. L. 1966. *De Ferri Metallographia*, Vol. 1. W. B. Sanders Company, Philadelphia.

Onasch, C. M. 1986. Ability of the Fry method to characterize pressure-solution deformation. *Tectonophysics* **122**, 187–193.

Ramsay, J. G. 1967. *Folding and Fracturing of Rocks*. McGraw-Hill, New York.

Ramsay, J. G. & Huber, M. I. 1983. *Techniques of Modern Structural Geology*, Vol. 1: *Strain Analysis*. Academic Press, London.

Smith, S. S. 1964. Some elementary principles of polycrystalline microstructure. *Metall. Rev.* **9**, 1–48.

Thomas, G. B. 1967. *Elements of Calculus and Analytical Geometry*. Addison-Wesley, Menlo Park, California.